Astronomy & Astrophysics manuscript no. SOAP-T-final-online
November 7, 2012

© ESO 2012

arXiv:1211.1311v1 [astro-ph.EP] 6 Nov 2012

SOAP-T*: A tool to study the light-curve and radial velocity of a system with a transiting planet and a rotating spotted star

M. Oshagh[1,2], I. Boisse[1], G. Boué[1,3], M. Montalto[1], N. C. Santos[1,2], X. Bonfils[4], and N. Haghighipour[5]

[1] Centro de Astrofísica, Universidade do Porto, Rua das Estrelas, 4150-762 Porto, Portugal
email: `moshagh@astro.up.pt`
[2] Departamento de Física e Astronomia, Faculdade de Ciências, Universidade do Porto,Rua do Campo Alegre, 4169-007 Porto, Portugal
[3] Astronomie et Systèmes Dynamiques, IMCCE-CNRS UMR8028, Observatoire de Paris, UPMC, 77 Av. Denfert-Rochereau, 75014 Paris, France
[4] UJF-Grenoble 1 / CNRS-INSU, Institut de Plantologie et d'Astrophysique de Grenoble (IPAG) UMR 5274, Grenoble, F-38041, France
[5] Institute for Astronomy and NASA Astrobiology Institute, University of Hawaii-Manoa, 2680 Woodlawn Drive, Honolulu, HI 96822,USA

Received XXX; accepted XXX

ABSTRACT

We present an improved version of SOAP (Boisse et al. 2012) named "SOAP-T", which can generate the radial velocity variations and light-curves for systems consisting of a rotating spotted star with a transiting planet. This tool can be used to study the anomalies inside transit light-curves and the Rossiter-McLaughlin effect, to better constrain the orbital configuration and properties of planetary systems and active zones of their host stars. Tests of the code are presented to illustrate its performance and to validate its capability when compared with analytical models and real data. Finally, we apply SOAP-T to the active star, HAT-P-11, observed by the NASA Kepler space telescope and use this system to discuss the capability of this tool in analyzing light-curves for the cases where the transiting planet overlaps with the star's spots.

Key words. methods: numerical- planetary system- techniques: photometry, Radial Velocity - Stellar activity

1. Introduction

Stellar spots and plages, combined with the rotation of the star, can mimic periodic Radial Velocity (hereafter RV) signals which may lead to false positives in the detection of a planet (Queloz et al. 2001; Bonfils et al. 2007; Huélamo et al. 2008; Boisse et al. 2009, 2011). Furthermore, the overlap of the planet and the active zones on the surface of a star can create anomalies inside the transit light curve that cause difficulties in constraining the depth of transit and as a result, the radius of the planet (Rabus et al. 2009). These anomalies can also lead to false positives in the detection of non-transiting planets by the transit timing variation method (Oshagh et al. 2012; Sanchis-Ojeda et al. 2011).

The stellar spots may provide important information about the orbital configuration of the star's planetary system. One quantity that is particularly interesting is the angle of stellar spin axis with respect to the orbital plane of the planet. There are two methods to measure this spin-orbit angle: the Rossiter-McLaughlin (hereafter RM) effect, which is based on the RV variations of the star during the planet's transit (e.g., Ohta et al. 2005; Winn et al. 2005; Narita et al. 2007; Hébrard et al. 2008; Triaud et al. 2009, 2010; Winn et al. 2010; Hirano et al. 2011), and the study of the anomalies inside the transit light-curve due to an overlap of the transiting planet with an active zone of its host star. If long-term and continuous observations of a star in photometry are accessible (e.g., target stars of the Kepler telescope), we will be able to detect the evolution of these anomalies inside transits and use them to determine the spin-orbit angle, inclination of the stellar spin axis, and the configuration of stellar spots on the surface of the star (longitude, latitude, and size) (Nutzman et al. 2011; Désert et al. 2011; Sanchis-Ojeda & Winn 2011; Sanchis-Ojeda et al. 2012). Measuring the angle between stellar spin axis and orbital plane, can give us a better understanding of the configuration of the planetary system as well as its formation, dynamical evolution, and possible migration (e.g., Queloz et al. 2000; Ohta et al. 2005;

---

* The tool's public interface is available at http://www.astro.up.pt/resources/soap-t/

Winn et al. 2005; Fabrycky & Winn 2009; Triaud et al. 2010; Morton & Johnson 2011; Hirano et al. 2012).

In this paper, we present a new tool for studying systems consisting of a rotating star with active zones and a transiting planet. The code, named "SOAP-T" generates synthetic radial velocity variations and produces light-curves for the system as functions of the stellar rotation phase. This tool is fast and as such can be utilized to simulate different possibilities for different initial configuration in order to find the best solution for inverse problems.

We describe SOAP-T in section 2. We will explain its software platform, language, input parameters, methodology, implementation, and output quantities. In section 3 we present several tests of this software to demonstrate its capabilities. Section 4 has to do with applying SOAP-T to the particular case of HAT-P-11 and comparing its result with the result of Sanchis-Ojeda & Winn (2011). We use this comparison as a demonstration of the capability of SOAP-T in analyzing the case where the planet and spot are overlapping. In the last section, we discuss other possible applications of SOAP-T and conclude this study by presenting its future improvements.

2. Software description

SOAP-T has been developed based on the already published code SOAP (Boisse et al. 2012) [http://www.astro.up.pt/soap/] that simulates spots and plages on the surface of a rotating star. We refer the reader to Boisse et al. (2012) for more details. The code in SOAP-T is written in Python with calls to functions written in C in order to make the code faster.

2.1. Inputs

The code requires initial conditions which can be assigned by the user in an input configuration file "driver.cfg".

The details of the initial parameters for the rotating spotted star can be found in Boisse et al. (2012). Here we explain the extra parameters that are required by SOAP-T.

Stellar parameters: One new feature of SOAP-T compared to SOAP is the implementation of the quadratic limb darkening (Mandel & Agol 2002) (SOAP considered the linear limb darkening for the star)

$$I(r) = 1 - \gamma_1(1-\mu) - \gamma_2(1-\mu)^2, \qquad \gamma_1 + \gamma_2 < 1. \tag{1}$$

In this equation, r is the normalized radial coordinate on the disk of the star, $I(r)$ is the specific intensity defined to reach its maximum 1 at the center of the star ($r = 0$) and its minimum at the star's limb, and $\mu = \cos\theta = (1-r^2)^{1/2}$ where θ is the angle between the normal to the surface and the observer. As shown by equation (1), the input parameters require two coefficients of quadratic limb darkening (γ_1 and γ_2).

Spot parameters: The number of spots is another important parameter. Unlike in SOAP where the number of spots could be up to 4, it is possible to choose up to 10 spots in SOAP-T.

Planet parameters:

Users are able to set the initial orbital configuration of the planet by selecting the following quantities: initial value of the planet's orbital period (P_{orb}), the time of its periastron passage (T_0), its initial orbital phase (PS_0), eccentricity (e), semimajor axis (a), argument of periastron (ω), inclination with respect to the line of sight (i), as well as the planet's radius (R_{planet}) and the angle between the stellar spin axis and the normal to the orbit of the planet projected on the $y-z$ plane. We denote this angle by λ.

2.2. Detail description of computation

We restate here from Boisse et al. (2012) that the rotating spotted star is centered on a grid of $grid \times grid$ cells on a y-z plane. The cells take their y and z values between -1 and 1, normalized to the stellar radius. Each grid cell (p_y, p_z) contains a flux value and a CCF (cross correlation function). Our goal in this section is to describe 1) how we add a planet to the rotating spotted star, 2) how we compute its impact in photometry and in RV, and 3) how we incorporate the overlap between the stellar inhomogeneities and the planet.

To determine the effect of a planet on the RV and flux of a non-spotted star in each phase step, the code first checks whether the planet is in the foreground or the background with respect to the star. For that reason, in the first step, SOAP-T calculates the position of the planet for each time step. Since the output of the code is in the stellar rotational phase, the code uses the following equation to convert stellar rotation phase into time

$$T = (PS + PS_0) \times P_{rot}. \tag{2}$$

The quantity PS is the stellar rotation phase which can be between 0 and 1, PS_0 is the planet's orbital initial phase which defines the initial position of the planet, and $P_{\rm rot}$ is the stellar rotation period in days. This equation is only valid for stellar rotation periods larger than the orbital period of the planet, which should be true for the most cases of transiting extrasolar planetary systems.

In order to determine the planet's position, the code has to calculate λ. As explained above, λ is the angle between the stellar spin axis (denoted by $\hat{n}_*$) projected on the $y-z$ plane and the unit vector normal to the plane of the planet's orbit (shown by $\hat{n}_p$ in figure 1) also projected on the same plane. The coordinates of vector $\hat{n}_*$ are determined using

$$\hat{n}_* = R_x(\psi_*)R_y(i_*)\begin{pmatrix}1\\0\\0\end{pmatrix} = \begin{pmatrix}\cos i_*\\ \sin i_* \sin\psi_*\\ -\sin i_* \cos\psi_*\end{pmatrix}, \tag{3}$$

where (ψ_*) is the longitude of stellar spin, (i_*) is the star's inclination, and R_x and R_y are the rotation matrices around the x and y axes. The coordinates of the normal vector $\hat{n}_p$ are also determined in the same fashion using the planet's longitude of ascending node (Ω) and orbital inclination (i) as

$$\hat{n}_p = R_x(\Omega)R_y(i)\begin{pmatrix}1\\0\\0\end{pmatrix} = \begin{pmatrix}\cos i\\ \sin i \sin\Omega\\ -\sin i\cos\Omega\end{pmatrix}. \tag{4}$$

The angle λ is then calculated using $\lambda = \Omega - \psi_*$. The code, subsequently, aligns the projected stellar spin axis with the z direction by setting $\psi_* = 180°$ and uses the longitude of the ascending node of the planet $\Omega = 180 + \lambda$ to calculate the coordinates of its position vector (see section 4 and equations 53-55 in Murray & Correia 2011 for more details). At each stellar phase step, the position vector of the planet ($\mathbf{D}$) is given by

$$\mathbf{D} = r_p\begin{pmatrix}\sin i\sin(\omega+f)\\ -\cos\lambda\cos(\omega+f)+\sin\lambda\cos i\sin(\omega+f)\\ -\sin\lambda\cos(\omega+f)-\cos\lambda\cos i\sin(\omega+f)\end{pmatrix}. \tag{5}$$

In equation (5)

$$r_p = \frac{a(1-e^2)}{1+e\cos f}, \tag{6}$$

where r_p is the distance between the stellar center and the center of planet, and

$$f = 2\tan^{-1}\left[\left(\frac{1+e}{1-e}\right)^{1/2}\tan\left(\frac{E}{2}\right)\right] \tag{7}$$

is the true anomaly of the planet. To calculate f, for small eccentricity, the code uses Kepler's equation

$$E = M + \frac{e\sin M - M}{1-e\cos M}, \tag{8}$$

where $M = 2\pi(T-T_0)/P_{orb}$ is the mean-anomaly of the planet's orbit (e.g. Ohta et al. (2005); Murray & Correia (2011)) (see Figure 1, a schematic view of a planetary system).

If the planet is in the foreground ($\mathbf{D}_x > 0$), the code checks if the planet is inside the stellar disk or outside by comparing the projected distance of the planet's center to the stellar center with the radius of star ($|\mathbf{D}| < R_*$). If the planet is inside, the code resolves the area of the grid where the planet is located and establishes an area around the planet where it will focus the subsequent calculations. This area is then scanned to determine whether each grid cell is located inside or outside the stellar disk (especially in the case where the planet is on the stellar limb), and if this grid cell belongs to the planet's disk, the code determines the location by calculating the distance of the grid cell to the center of planet and comparing it with planet's radius. Assuming that a grid cell is located inside the stellar disk and also belongs to the planet's disk, its CCF is modeled by a Gaussian with a width and amplitude given by the input parameters and doppler-shifted according to the projected stellar rotation velocity weighted by the quadratic limb-darkening law. This CCF value will then be removed from the total CCF of the rotating non-spotted star. For the same grid cell, the values of the flux can be calculated using only on the quadratic limb-darkening law. The code also removes the flux value of that cell from the total flux of the rotating spotted star.

In the next step, the code adds a planet to the rotating spotted star in order to calculate the effect of both the planet and the spots on the RV and flux at the same time. In the case that the spot is not partly covered by the planet, the procedure is as explained below. The code

- determines the position of the spot,
- determines the position of the planet,
- applies inverse rotation to the spot to bring it along the line of sight,
- scans the region of the spot's position to identify the grid cells that belong to the spot's disk area,
- sums up the CCF and flux of all cells inside the spot and removes them from the total flux and CCF of the non spotted-star [see figure 4 of Boisse et al. (2012) for the inverse rotation and also for more details on spots calculation],
- scans the region of the planet's position to determine the grid cells that are inside the disk of the planet,
- calculates the sum of the CCF and flux for those grid cells inside the transiting planet and removes them from the total flux and CCF of the spotted star.

The complexity arises from the overlapping of the transiting planet with a spot on the surface of the star. In this case, the code considers those parts of the spot whose distances to the center of the planet are smaller than the planet's radius as the overlapped area. Those points will not be scanned during the spot scanning process. As a consequence, they will skip the rest of procedure for CCF and flux of spot and removal from total CCF and flux. This procedure is able to produce those positive "bump" anomalies inside the transit light curve that are due to the reduction in the loss of light. The schematic view of the system which is simulated by SOAP-T is shown in Figure 2.

2.3. Outputs

The code returns the results of its simulation into the output file "output.dat". The output file contains four columns that represent stellar phase, flux, RV and BIS (the bisector span), respectively. These quantities can be plotted directly by SOAP-T as functions of the stellar rotation phase. Similar to SOAP, the stellar phase step can

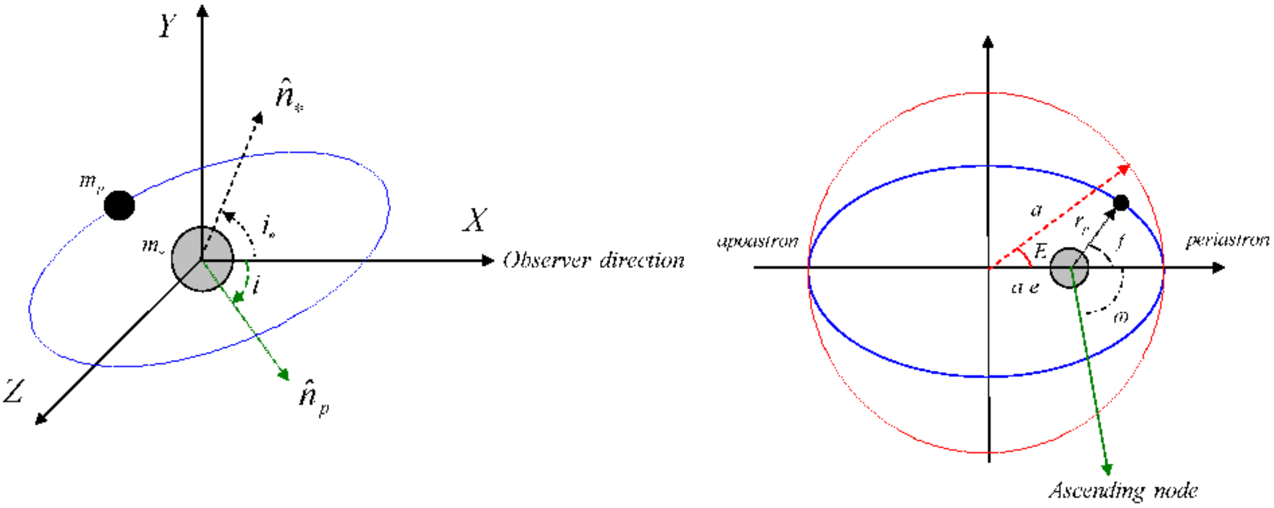

Fig. 1. Left: Schematic configuration of the stellar spin axis and planetary orbital plane. The vector $\hat{n}_p$ is the normal unit vector of the planetary orbital plane, the vector $\hat{n}_*$ is the stellar spin axis, and i_* is the stellar inclination. We denote the angle between the projected stellar spin axis and the projected normal unit vector of the planetary orbital plane on the $y-z$ plane with λ (not shown here). Right: Schematic view of planetary orbit from above the orbital plane, the star is the gray circle and the planet is the black full circle. See Section 2 for more details on the symbols.

be chosen in two ways, first by selecting the constant fraction of the phase between 0 to 1, or by uploading the wanted phase values in the *ph_in* file. The flux values correspond to the photometry of the system (the total flux of system), and they are normalized to the maximum value of total flux during the stellar rotation phase. The RV values are obtained by fitting a Gaussian function to each total CCF [see more details in Boisse et al. (2012)]. We note here that each total CCF is also normalized to its maximal value. We refer the reader to Queloz et al. (2001) for details on BIS calculations.

3. Tests

To check the capability of SOAP-T and the validity of its result, we preformed several tests to compare its outcome with theoretical models and real observations. Tests related to the effects of spots on the RV and flux signals have been presented and explained in Boisse et al. (2011, 2012). In this section, we test the validity of the results for the photometry and RV with a transiting planet around both a non-spotted and a spotted star.

To begin with, we consider a system consisting of a non-spotted star with a transiting planet. The purpose of this test is to determine whether the code can reproduce the light curve of a star with a transiting planet as obtained from the theoretical model of Mandel & Agol (2002). We select various initial conditions including a star without any limb darkening, or with linear or quadratic limb darkening. As shown in Figure 3, the results obtained from SOAP-T are in strong agreement with the results obtained from the theoretical model based on the formalism presented by Mandel & Agol (2002). The latter implies that SOAP-T can be used reliably to characterize the light-curve of a transiting planetary system.

In a second test, we examined the RVs obtained using SOAP-T during the transit of a planet in front of a non-spotted star. We applied SOAP-T to the system of WASP-3 which is known to harbor a planet with a misalignment between its orbital plane and stellar spin axis (see the parameters of WASP-3 system in the Table 1). The RV observation data of WASP-3 during its transits were taken from Simpson et al. (2010) (it was observed with the SOPHIE spectrograph at Haute-Provence Observatory). We fitted the RVs produced by SOAP-T to the observational data and compared the results with those of Simpson et al. (2010). We only allowed stellar rotation velocity ($v \sin i$) and misalignment angle (λ) to vary as free parameters, and kept all other parameters constant and equal to their values reported by Gibson et al. (2008) and Simpson et al. (2010) (see Table 1).

The best fit result obtained using SOAP-T corresponds to $\lambda = 20.0^\circ \pm 3.3^\circ$ and $v \sin i = 13.31 \pm 0.45\,\mathrm{km s^{-1}}$ with $\chi^2_{\rm red} = 0.9308$. We obtained the error bars of these measurements using the bootstrap method (Wall & Jenkins 2003). The value of the misalignment angle (λ) is consistent with the value reported by Simpson et al. (2010) ($13^\circ \pm^{9^\circ}_{7^\circ}$) within 1σ. Note that the error bars obtained with SOAP-T are more than twice smaller than those derived by Simpson et al. (2010). We assume that this could be due to smaller number of free parameters in our fitting procedure, otherwise it might be also due to the fact that SOAP-T has been developed to reproduce exactly the analysis routine of RV measurements and is thus closer to the observations when compared to the result of the analytical formula used by Simpson et al. (2010) (Boué et al. 2012). Indeed, we obtained also a better agreement between the projected stellar rotation velocity ($v \sin i$) and the value obtained by spectroscopic broadening measurements ($13.4 \pm 1.5 kms^{-1}$). For comparison, Simpson et al.

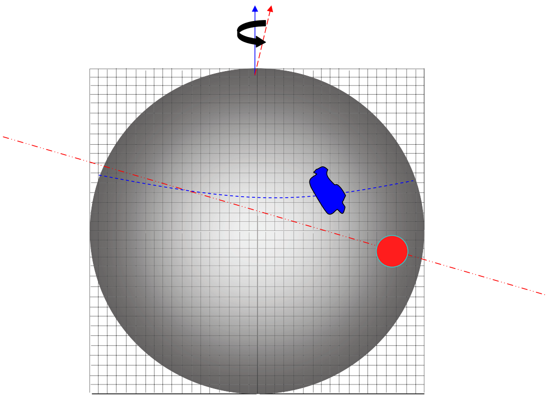

Fig. 2. Schematic view of stellar spot and the transiting planet in simulations by SOAP-T.

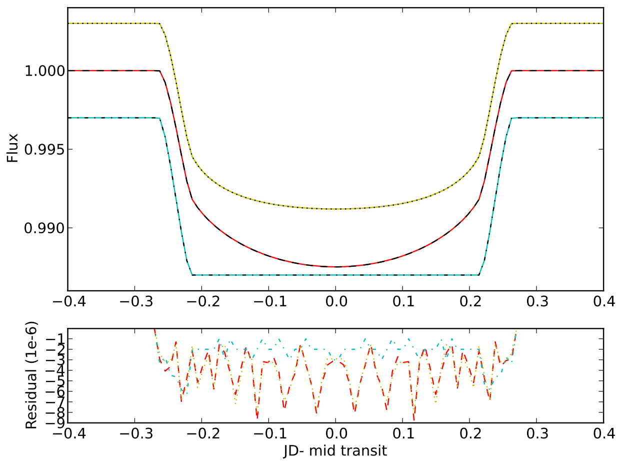

Fig. 3. Comparing the photometric results of SOAP-T and the theoretical model of a transiting planet over a non-spotted star (Mandel & Agol 2002). The cyan, red, and yellow lines show SOAP-T's results for a star without limb darkening, a star with linear limb darkening ($\gamma_1 = 0.6$), and a star with quadratic limb darkening ($\gamma 1 = 0.29$ and $\gamma 2 = 0.34$), respectively. The dash-dotted line, dashed line, and the dotted line show the corresponding results using the mechanism by Mandel & Agol (2002).

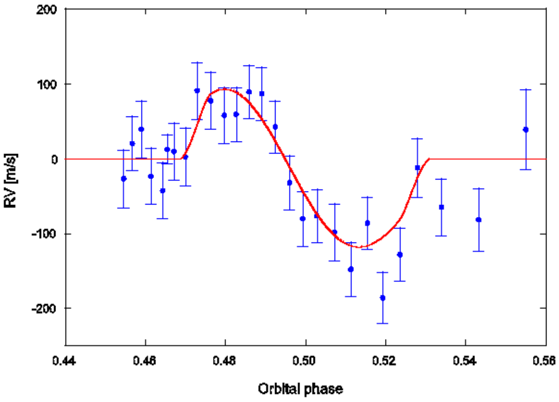

Fig. 4. RV observations of WASP-3 during transit of WASP-3b (RM effect) minus Keplerian motion, which are blue dots (Simpson et al. 2010), overplotted with the best fit of RV signals obtained from SOAP-T, which is red line.

(2010) obtained $v \sin i = 19.6 \pm^{2.2}_{2.1} \, kms^{-1}$. Figure 4 shows the result of the best SOAP-T RV's fit and the observation of RM effect of WASP-3.

Finally, since there is no theoretical model for the case where a transiting planet and star spots overlap, to evaluate the performance of SOAP-T in this case, we compared the photometric result of SOAP-T with the results reported in the literature for the real observation of HAT-P-11 by the Kepler space telescope. We will explain this test and its applications in the next section.

4. Application of SOAP-T to HAT-P-11

HAT-P-11 is a 6.5 Gyr bright (V=9.6) K4 star with a mass of 0.81 $M_{\odot}$ and radius of 0.75 $R_{\odot}$. At a distance of 38 pc, this star hosts a transiting Neptune-sized planet with a mass of 0.081 M_{Jup} and radius of 0.422 R_{Jup} (Bakos et al. 2010). HAT-P-11b has a period of 4.887 days and revolves around its central star in an orbit with a semimajor axis of 0.053 AU and an eccentricity of $e = 0.198$. More details of the parameters of this planet and its host star can be found in Table 2.

Studies of the HAT-P-11 planetary system have shown extreme misalignment of the projected angle between the stellar spin axis and the planet's orbital plane ($\lambda = 103^{\circ} \pm^{26^{\circ}}_{10^{\circ}}$) through RM effect (Winn et al. 2010).

HAT-P-11 (KOI-3) was used as one of the calibration target stars for the Kepler space telescope and has been observed throughout Kepler's mission in both short and long cadences. The high precision photometry of this star has revealed some features inside its transit light curve and has also shown a large modulation outside of transits. The anomalies inside the transit light curve of HAT-P-11 can be attributed to the overlapping of the transiting planet with active zones on the surface of the star (Sanchis-Ojeda & Winn 2011). The recurrence (or not) of these anomalies can be used to put an upper limit on the stellar obliquity. Recently Sanchis-Ojeda & Winn (2011) carried out a purely photometric study of this system based on the observation of photometric anomalies inside the transit light curve using the Kepler public data Q0-Q2 and showed that no recurrence of anomalies exists in two closely spaced transits in the Kepler data of HAT-P-11. They considered this result as evidence of misalignment of the stellar spin axis with respect to orbital plane. Fortunately, these authors were able to detect a feature with two peaks in the folded light curve of 26 transits of

Table 1. The stellar and planet's parameters of the WASP-3 system (Gibson et al. 2008; Simpson et al. 2010).

Parameter	Value	Uncertainty
Stellar parameters		
$R_\star(R_\odot)$	1.31	$\pm^{0.05}_{0.07}$
Linear limb darkening coefficient	0.69	-
Stellar inclination (deg)	90	-
Spectroscopic stellar rotation velocity $v\sin i(kms^{-1})$	13.4	±1.5
Planet parameters		
Planet to star radius ratio (R_p/R_*)	0.1013	$\pm^{0.0014}_{0.0013}$
Period (days)	1.846835	±0.000002
Eccentricity	0	-
Scaled Semimajor axis (a/R_*)	5.173	$\pm^{0.246}_{0.162}$
Orbital inclination (deg)	84.93	$\pm^{1.32}_{0.78}$
Projected spin-orbit misalignment angle(deg)	13	$\pm^{9}_{7}$

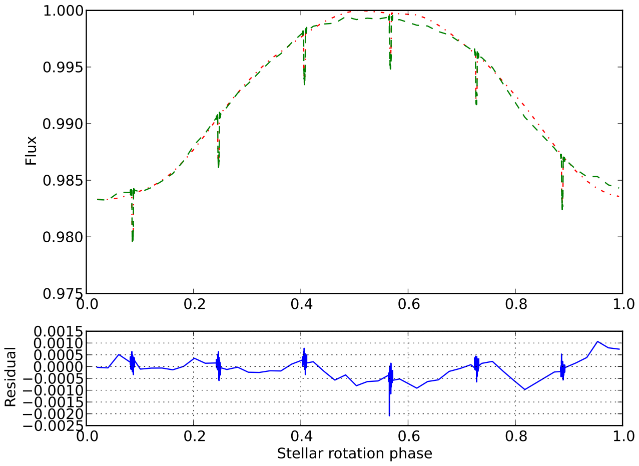

Fig. 5. Comparing the best fit model to the transit photometry of HAT-P-11 using SOAP-T and the Kepler observation of HAT-P-11 for one period of stellar rotation. Red (dash-dotted) line shows SOAP-T's photometric result for an edge-on solution and green(dashed) line correspond to HAT-P-11 observation. The blue (solid) line in the bottom panel shows the residual.

this star which could be interpreted as evidence for the existence of two long lived spot belt regions on the star. By using a simple geometric model, these authors arrived at two solutions for the stellar obliquity; an edge-on solution that is in good agreement with the result of Winn et al. (2010) through the RM study, and an alternative solution in which the star is seen almost pole-on. The method used by Sanchis-Ojeda & Winn (2011) also allowed these authors to put some constraints on the position (latitude) and size of the active zones on the surface of star (see details of parameters for two solutions in Table 3).

Here we present the results of the application of SOAP-T to HAT-P-11 in order to reproduce the light curve of this star over one stellar rotation. The rotation period of this star contains six transits.

Since the inside transit anomalies carry more information about the configuration of a planetary system, we decided to give more weight to these points in our study. We, therefore, performed a regular sampling to reduce the number of points outside of the transit light curve. One point was taken from each 300 points in the light curve out side the transit. This process reduced the running time of the code significantly.

4.1. HAT-P-11 Edge-on solution

In this section, we consider the system to be edged-on and choose all initial parameters of the star, planet, and spots (except the number of spots and their longitude) from the values reported by Sanchis-Ojeda & Winn (2011). The spot's brightness are fixed to zero. The details of initial conditions are listed in Table 3. To reproduce all the features in the light curve, both inside and outside the transit, we limited the latitude and the size of the spots to the range reported by Sanchis-Ojeda & Winn (2011). The spots's radius are equal to the half-width of the active zone which correspond to $R_{spot} = 0.08R_*$). However, we allowed the number of spots and their longitudes to vary as free parameters between 0-10 and $0° - 360°$, respectively. The best fit to the observations ($\chi^2_{red} = 7.356$) was obtained with eight spots on the surface of the star. Figure 5 shows the best result of SOAP-T photometry overplotted with the real observation of HAT-P-11 during one stellar period. Figure 6 shows more details of the inside of each transit and the results obtained from SOAP-T after normalizing both flux values to one. As shown in both figures, SOAP-T could manage to reproduce all the inside transit anomalies and also the out side transit variation. We note here that the results of Sanchis-Ojeda & Winn (2011) were obtained by considering the inside transit anomalies. These authors did not consider the outside features of the light curve. However, using SOAP-T we were able to study the entire light-curve, both inside transit and outside, at the same time. We note that here we do not intend to confirm the results of Sanchis-Ojeda & Winn (2011). We only use the similarities between the results obtained from SOAP-T photometry (e.g. position and size of spots, stellar inclination and spin-orbit misalignment angle) and the results by these authors as a proof of the validity of SOAP-T's capability in simulating the case of spot and planet overlapping.

Table 2. The stellar and planet's parameters of the HAT-P-11 system (Bakos et al. 2010; Sanchis-Ojeda & Winn 2011).

Parameter	Value	Uncertainty
Star parameters		
$M_\star(M_\odot)$	0.81	$\pm^{0.02}_{0.03}$
$R_\star(R_\odot)$	0.75	±0.02
Stellar rotation period (days)	30.5	$\pm^{4.1}_{3.2}$
Age (Gyr)	6.5	$\pm^{5.9}_{4.1}$
Distance (pc)	38.0	±1.3
Linear limb darkening coefficient	0.599	±0.015
Quadratic limb darkening coefficient	0.073	±0.016
Planet parameters		
$M_P(M_{Jup})$	0.081	±0.009
Planet to star radius ratio (R_p/R_*)	0.05862	±0.00026
Orbital period (days)	4.8878049	±0.0000013
Scaled Semimajor axis (a/R_*)	15.6	±1.5
Eccentricity	0.198	±0.046

Table 3. Parameters of the HAT-P-11 system for different solutions reported by Sanchis-Ojeda & Winn (2011).

Parameter	Value	Uncertainty
Edge-on solution		
Projected spin-orbit misalignment angle λ (deg)	106	+15/-12
Stellar inclination i_s (deg)	80	+4/-3
Latitude of active zone (deg)	19.7	+1.5/-2.2
Half-width of active zone (deg)	4.8	+1.5/-1.8
Pole-on solution		
Projected spin-orbit misalignment angle λ (deg)	121	+24/-21
Stellar inclination i_s (deg)	168	+2/-5
Latitude of active zone (deg)	67	+2/-4
Half-width of active zone (deg)	4.5	+1.6/-1.9

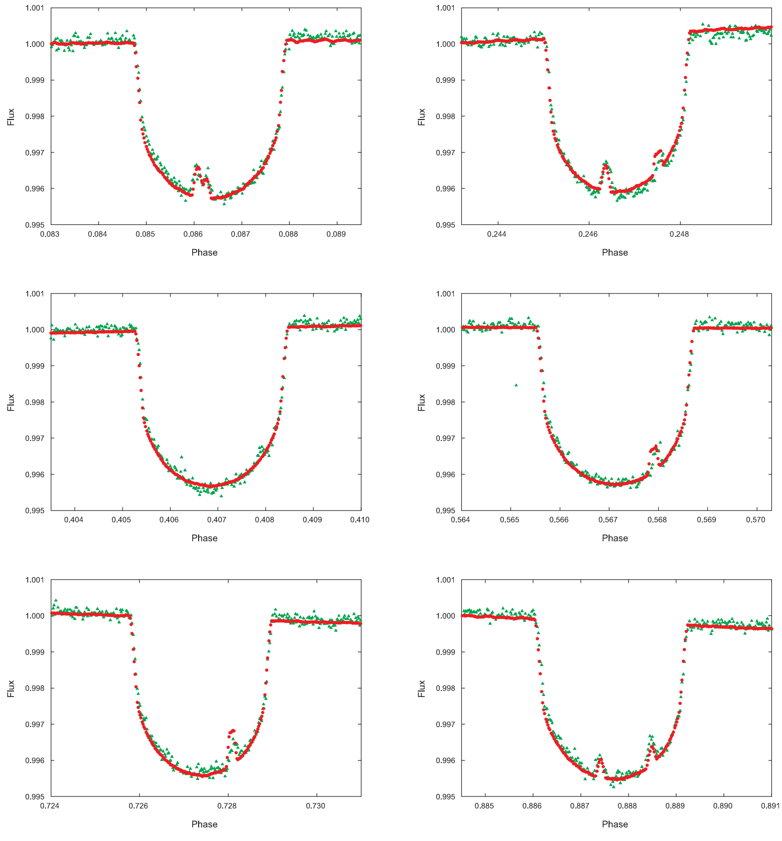

Fig. 6. Zoom on the six transits of HAT-P-11 in the figure 5. The flux values are normalized to one for both observation and SOAP-T. Red dot represent the SOAP-T photometric result and green triangles are observed flux of HAT-P-11.

4.2. HAT-P-11 pole-on solution

In this section, we examine the pole-on model for the system proposed by Sanchis-Ojeda & Winn (2011). We note that here we explore which configuration of spot on the surface of the star would be able to generate the out of transits variation and we did not attempt to reproduce the inside transit features. We generated the light curve of HAT-P-11 using SOAP-T photometry and the parameters of the pole-on model given by these authors. (see the details of parameters in Table 3). Since the pole-on solution presented by Sanchis-Ojeda & Winn (2011) is only nearly pole-on (i.e., the angle of misalignment is $\sim 168°$), some spots located close to the equator of the star can produce large variations outside the transit by disappearing from the view for a small part of the rotation period. We investigated the effect of different possible sizes of the spots that were located in different latitudes. Our analysis showed that the optimized result, whose outside-transit profile is similar to that from the observation, has to have a spot on $20°$ or $60°$ latitude with a size equal to $0.2R_*$ (see Figure 7). Since the brightness of spot is fixed to zero, it is the minimal size of the spot. For a star with a similar spectral type as HAT-P-11 (i.e., K), this is a very large spot. Although spots with very large sizes have been detected on K stars (Strassmeier 1999), this situation is unlikely for HAT-P-11.

5. Conclusion and Perspective

In this paper, we introduced a new software package that can be used to produce the photometric and RV signals of a system consisting of a rotating spotted star and a transiting planet where the spots and planet overlap. We tested the capability of our code by comparing its results with theoretical models and the results of observations. We used the HAT-P-11 system and demonstrated that when using the edge-on model of Sanchis-Ojeda & Winn (2011), SOAP-T is capable of reproducing the same features as obtained from observations for the outside of transits as well as the anomalies inside the transits. We also showed that the reconstruction of the large modulation of the outside transit of HAT-P-11 with the pole-on model of Sanchis-Ojeda & Winn (2011) requires an assumption on the size of spot on the star which may not be realistic.

In using SOAP-T, the number of free parameters of a system that can be chosen by the user is large. In general, for a system consisting of a rotating star with one spot and a planet transiting, there are 18 free parameters. As a result, for a system where parameters are not constrained (e.g., by observation), the finding of the best solution that fits real observation becomes a complicated task. The minimization of the reduced chi-squared (the indicator of goodness of the fit) in this case requires the exploration of a large parameter space. A simple griding of this space turns the calculations into a time consuming process which may result in the finding of local minima instead of a global minimum. Efforts are currently underway to investigate different optimization strategies which can lead to faster and more secure determination of a global minimum.

Acknowledgements. We acknowledge the support by the European Research Council/European Community under the FP7 through Starting Grant agreement number 239953, and by Fundação para a Ciência e a Tecnologia (FCT) in the form of grant reference PTDC/CTE-AST/098528/2008 and SFRH/BPD/81084/2011. NCS also acknowledges the support from FCT through program Ciência 2007 funded by FCT/MCTES (Portugal) and POPH/FSE (EC). NH acknowledges support from the NASA/EXOB program through grant NNX09AN05G and from the NASA Astrobiology Institute under Cooperative Agreement NNA09DA77 at the Institute for Astronomy, University of Hawaii.

Some of the data presented in this paper were obtained from the Multimission Archive at the Space Telescope Science Institute (MAST). STScI is operated by the Association of Universities for Research in Astronomy, Inc., under NASA contract NAS5-26555. Support for MAST for non-HST data is provided by the NASA Office of Space Science via grant NAG5-7584 and by other grants and contracts.

References

Bakos, G. Á., Torres, G., Pál, A., et al. 2010, ApJ, 710, 1724
Boisse, I., Bonfils, X., & Santos, N. C. 2012, A&A, 545, A109
Boisse, I., Bouchy, F., Hébrard, G., et al. 2011, A&A, 528, A4
Boisse, I., Moutou, C., Vidal-Madjar, A., et al. 2009, A&A, 495, 959
Bonfils, X., Mayor, M., Delfosse, X., et al. 2007, A&A, 474, 293
Boué, G., Montalto, M., Boisse, I., Oshagh, M., & Santos, N. 2012, Submitted to A&A
Désert, J.-M., Charbonneau, D., Demory, B.-O., et al. 2011, ApJS, 197, 14
Fabrycky, D. C. & Winn, J. N. 2009, ApJ, 696, 1230
Gibson, N. P., Pollacco, D., Simpson, E. K., et al. 2008, A&A, 492, 603
Hébrard, G., Bouchy, F., Pont, F., et al. 2008, A&A, 488, 763
Hirano, T., Sanchis-Ojeda, R., Takeda, Y., et al. 2012, ApJ, 756, 66
Hirano, T., Suto, Y., Winn, J. N., et al. 2011, ApJ, 742, 69
Huélamo, N., Figueira, P., Bonfils, X., et al. 2008, A&A, 489, L9
Mandel, K. & Agol, E. 2002, ApJ, 580, L171
Morton, T. D. & Johnson, J. A. 2011, ApJ, 729, 138
Murray, C. D. & Correia, A. C. M. 2011, Keplerian Orbits and Dynamics of Exoplanets, ed. S. Piper, 15–23
Narita, N., Enya, K., Sato, B., et al. 2007, PASJ, 59, 763
Nutzman, P. A., Fabrycky, D. C., & Fortney, J. J. 2011, ApJ, 740, L10
Ohta, Y., Taruya, A., & Suto, Y. 2005, ApJ, 622, 1118

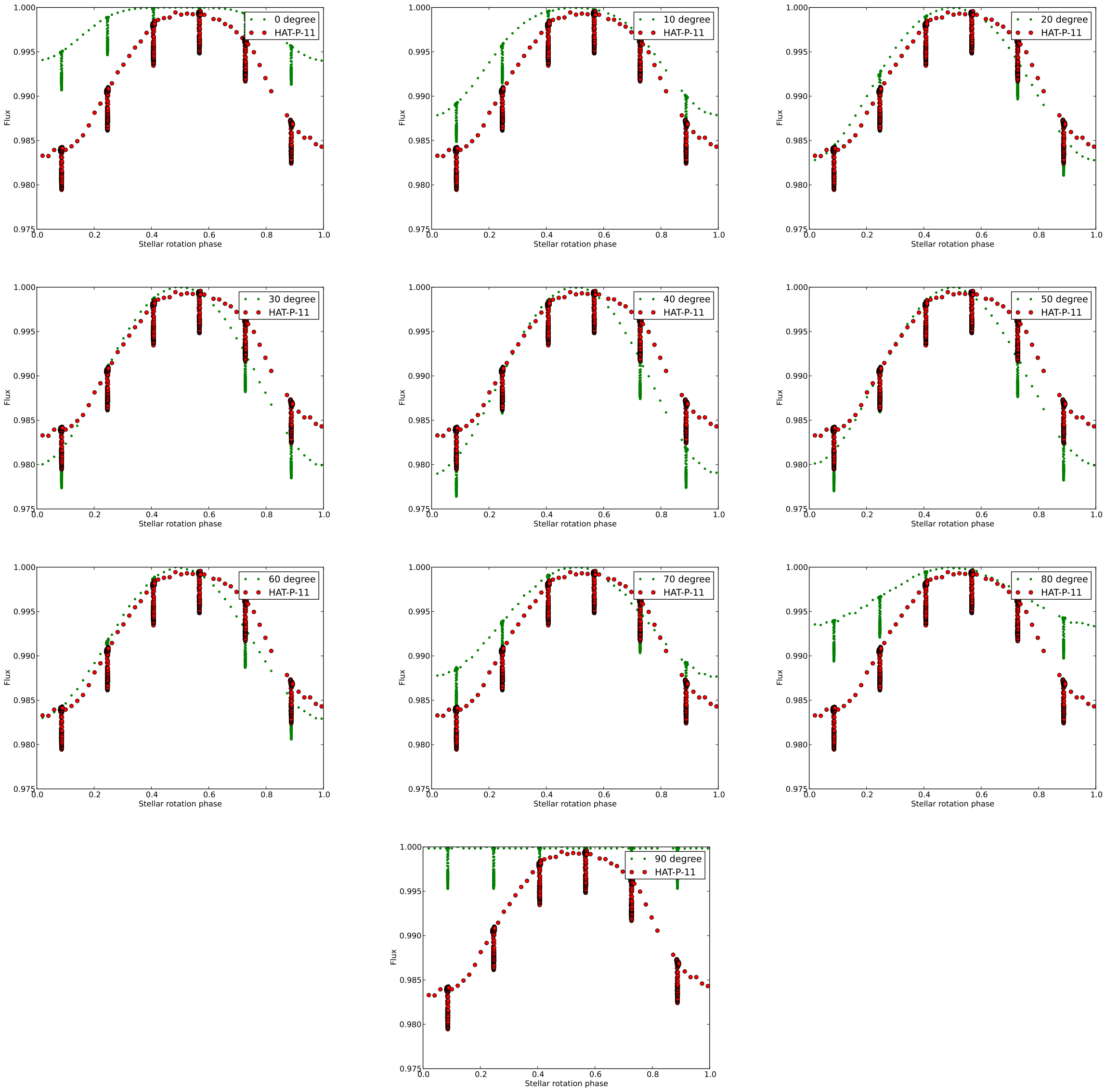

Fig. 7. Comparing SOAP-T's photometric result with the observation of HAT-P-11 for the pole-on model of Sanchis-Ojeda & Winn (2011). Each panel shows different values for the latitude of one spot with the size of 0.2 radius of star. Green dot is the SOAP-T photometric result and red circle is the observation of HAT-P-11.

Oshagh, M., Boué, G., Haghighipour, N., et al. 2012, A&A, 540, A62

Queloz, D., Eggenberger, A., Mayor, M., et al. 2000, A&A, 359, L13

Queloz, D., Henry, G. W., Sivan, J. P., et al. 2001, A&A, 379, 279

Rabus, M., Alonso, R., Belmonte, J. A., et al. 2009, A&A, 494, 391

Sanchis-Ojeda, R., Fabrycky, D. C., Winn, J. N., et al. 2012, Nature, 487, 449

Sanchis-Ojeda, R. & Winn, J. N. 2011, ApJ, 743, 61

Sanchis-Ojeda, R., Winn, J. N., Holman, M. J., et al. 2011, ApJ, 733, 127

Simpson, E. K., Pollacco, D., Hébrard, G., et al. 2010, MNRAS, 405, 1867

Strassmeier, K. G. 1999, A&A, 347, 225

Triaud, A. H. M. J., Collier Cameron, A., Queloz, D., et al. 2010, A&A, 524, A25

Triaud, A. H. M. J., Queloz, D., Bouchy, F., et al. 2009, A&A, 506, 377

Wall, J. V. & Jenkins, C. R. 2003, Practical Statistics for Astronomers (Cambridge University Press)

Winn, J. N., Johnson, J. A., Howard, A. W., et al. 2010, ApJ, 723, L223

Winn, J. N., Noyes, R. W., Holman, M. J., et al. 2005, ApJ, 631, 1215